Metrological evaluation of an AI-based vision computing model for crack detection on masonry structures

Giovanni Salerno[1*], *Maria Teresa* Calcagni[1], *Milena* Martarelli[1], and *Gian Marco* Revel[1]

[1]Università Politecnica delle Marche, 60131 via Brecce Bianche 12, Italy

Abstract. Ensuring the structural integrity of buildings is essential for their longevity and safety. Traditional methods of surface monitoring, crucial for detecting potential damages that could lead to structural failures, are often labour-intensive, subjective, and challenging to document comprehensively. This paper proposes an innovative, automated approach to address these challenges by leveraging advanced computer vision and artificial intelligence. The method focuses on the detection of cracks in masonry building elements, a common but critical indicator of building surface wear. Utilizing a robust AI model trained on a diverse dataset of real crack images, the crack area is identified, and the system is able to accurately determine crack dimensions, encompassing both width and length, by analysing the contour of this area. An analysis was carried out on synthetically generated images to determine which parameters most significantly affect the detection capabilities of the AI model, and validation of real crack images was performed. Our approach redefines building monitoring by combining the precision of machine learning and vision systems techniques with the strategic insights provided by a comprehensive platform, setting a new standard for structural health management in the construction industry.

1 Introduction

Masonry structures are an emblem of historical heritage and modern architectural innovation and face persistent maintenance challenges due to load and environmental exposure. These constructions, assembled from different materials such as brick, stone, or blocks, are prone to structural cracks, which may indicate underlying failures. Given the complexity of masonry models and the heterogeneity of materials, their maintenance requires not only an understanding of mechanical behaviour and degradation processes, but also periodic inspections by experts [1]. This necessity highlights the use of technically advanced methods to ensure their longevity and safety [2], supported by analytical tools like modelling strategies for computational analysis of masonry structures [3].

Over the years, many researchers have studied a wide variety of technological methodologies that could be leveraged to optimize Structural Health Monitoring (SHM),

* Corresponding author: g.salerno@staff.univpm.it

These proceedings are published with the support of EuLA.

employing them to address its various challenges. The importance of SHM cannot be underestimated, as it is directly related to the safety, durability, and functionality of built environments, requiring continuous adaptation and advancement of the methods used to perform it [4], [5].

From traditional mechanical testing, performed employing ground-level inspections [6], to tactile inspections using baskets, scaffolding, or rope [7]; progress has been made with sensor-based systems such as drones-based inspections [8], to the most advanced techniques such as the exploitation of artificial intelligence and machine learning models [9]. Indeed, the evolution of SHM techniques reflects a trajectory of innovation aimed at improving the accuracy, efficiency, and effectiveness of monitoring practices.

The focus of this research was to study the detection of cracks occurring on façades during their life cycle and to propose a valuable tool to be exploited for SHM. Valero et al. proposed a machine learning-based approach for defect detection and classification on masonry walls, starting with the acquisition of spatial data and moving on to segmentation, defect detection and classification [10]. Qiu et al. developed a method to identify cracks on tiled sidewalks using UAVs for data acquisition, comparing several versions of the YOLO model [11]. An automatic methodology for the detection and classification of cracks on masonry surfaces was developed using a convolutional neural network and transfer learning, obtaining satisfactory results [12]. Halle et al., developed a crack detection algorithm based on CNN. A dataset of 2542 masonry wall image patches, obtained in a controlled laboratory environment, was created for model training. Real-world and laboratory images were used for testing [13]. The usage of limited data for model training is crucial nowadays, Katsigiannis et al. developed a deep learning-based method using transfer learning for crack detection on masonry façades. The dataset used was composed of 700 images divided between training, validation, and testing [14]. Shamsabadi et al., proposed transformers-based models for crack detection, comparing them with CNNs generally used for this application, and obtained successful results [15]. Defect quantification, in addition to identification using segmentation techniques, is a key aspect. The study by Dang et al. presents models for crack recognition and length measurement on real cracks that appeared on masonry façades [16]. Another work focused on the evaluation of fissures arising on surfaces uses the U-Net model based on semantic segmentation for defect detection and assessment [17]. The study on the automatic selection of input parameters for Steger ridge detection inspired the measurement method presented in this paper [18]. The integration of artificial intelligence (AI) and computer vision has revolutionised traditional structural inspection methods, opening a new era of efficiency and reliability. Advances in image processing, machine learning and data analysis converge in cutting-edge systems designed for automatic detection of structural anomalies.

The objective of this study was not only to present a method for the recognition of cracks on a masonry element and to quantify their extension but also to assess its metrological performances through statistical analysis. An AI model was employed to obtain the segmentation of the defect in the image and, using a measurement algorithm, the thickness and length of the crack on the surface under investigation were quantified. To assess the uncertainty of the model related to different sources (crack orientation, image contrast, …), synthetic images of cracks on masonry were generated in order to create a distribution of the image population used for statistical analysis. Finally, the applicability of the method has been demonstrated on real masonry cases.

2 Materials and methods

2.1 Crack detection by AI model

The artificial intelligence model employed is a segmentation model designed to detect and segment the crack defect in the images. The model is based on the U-Net architecture, which was developed for precise image segmentation, and initially applied in the biomedical field [19]. It consists of a fully convolutional neural network, with a symmetric design: the encoding (or contracting) path and the decoding (or expanding) path. The first path uses repeated convolutions, activated by rectified linear units (ReLUs), and followed by max pooling operations to capture the wider context of the image. The decoding path progressively increase the resolution of abstract features and helps to accurately segment objects at several scales. The backbone used is efficientNet-b7. The model has been trained on a private dataset of 750 images of crack on different types of walls, both masonry and concrete, collected from ruined buildings and manually segmented for precise training. The dataset has been split into training, validation, and test subsets according to the ratio: 80%, 10%, 10%. The effectiveness of the model is evaluated using two primary metrics: the Intersection over Union (IoU) score (IoU $= \frac{TP}{TP + FP + FN}$ (1 IoU $= \frac{TP}{TP + FP + FN}$ (1)) and the model loss (Model Loss $= Dice\ Loss + Focal\ Loss$ (2)). The IoU score measures the accuracy of segmentation by calculating the area of overlap between the predicted segmentation and ground truth divided by the area of their union. A higher IoU score indicates superior segmentation performance.

$$IoU = \frac{TP}{TP + FP + FN} \quad (1)$$

Regarding model loss, a hybrid approach combining Dice Loss and Focal Loss was used to optimise the results. Dice Loss assesses the similarity between the predicted segmentation and ground truth, effectively addressing class imbalance issues in images [20]. Focal loss is intended to improve the model's focus on hard-to-classify pixels, thus refining the learning process in difficult areas of the images [21]. The total loss is computed as follows:

$$Model\ Loss = Dice\ Loss + Focal\ Loss \quad (2)$$

The training lasts 130 epochs, and after the final training session, the model metrics are reported in the Table 1.

Table 1. Model metrics.

IoU score	Model loss
0.991	0.135

The model predicts the segmentation of the crack, providing a value between 0 (crack) and 1 (not crack), with the threshold for image binarization of 0.5.

The predicted images are then used for the statistical evaluation of the generation variables, as explained in the next section.

2.2 Crack images generation and definition of evaluation metric

The masonry defect conditions considered for the generation of synthetic images are those that may most compromise defect identification during recognition. These conditions can be

considered as sources of uncertainty for the defect identification model, and can be related to two aspects:

1. the physics of the inspected element: crack thickness, mortar joint thickness (between the masonry units) and crack rotation angle with respect to the direction of the mortar joint
2. image quality, particularly the contrast between the defect and the background. This uncertainty source was modelled by adjusting the colour of the crack and the mortar joint colour.

Images of masonry walls were generated synthetically to systematically control variations in crack and mortar joint parameters, with the joints blurred to better replicate real-world conditions. An example of a synthetic image representing a crack on a masonry wall is depicted in Fig. 1, where the crack and mortar joint colour and thickness values are optimal for proper visualisation. The angle of crack rotation defined as the angle between the horizontal axis and the direction of the crack, is explained.

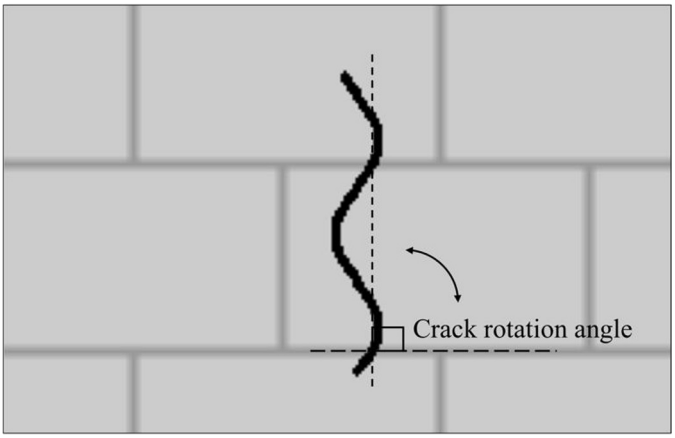

Fig. 1. Example of synthetic image for the model evaluation.

All images produced were analysed by the AI model to identify and segment the cracks, and the predicted masks were compared to the ground truth crack images to evaluate the effectiveness of the model in relation to the image and crack generation parameters. The metric used is the IoU (Intersection over Union) score, as the comparison is based on the crack segmentation.

A statistical analysis was performed to evaluate the influence of each parameter varied in the image generation on AI model identification.

The measurement algorithm, developed for crack width and length assessment, is applied to the predicted mask obtained by the AI model. Therefore, it is necessary to understand what parameters allow the model to perform best.

Table 2 shows the sources of uncertainty considered and their range of variation used for the statistical analysis.

Considering the grayscale colour bar shown in the Fig. 2, which has a range from 0 to 1, where 0 identifies black and 1 identifies white, a neutral, fixed colour of 0.8 was chosen for the masonry unit. Areas of shadow are often present along the gap. These shadow areas may appear darker because direct light does not fully reach that part of the surface, creating a visual contrast with the surrounding areas. For this reason, the crack has been assigned a range of values from 0 to 0.4. The joint, on the other hand, can be a mixture of lighter and

darker material, rarely reaching the same shade as the crack. In each case, all these variations were considered by selecting the range from 0.3 to 0.7.

Table 2. Uncertainty sources variation ranges.

Uncertainty sources	Variability range
Crack thickness	1 to 11 [pixels]
Mortar joint thickness	3 to 13 [pixels]
Crack colour	0 to 0.4
Mortar joint colour	0.3 to 0.7
Crack rotation angle (see Fig. 1)	0 to 90 [deg]

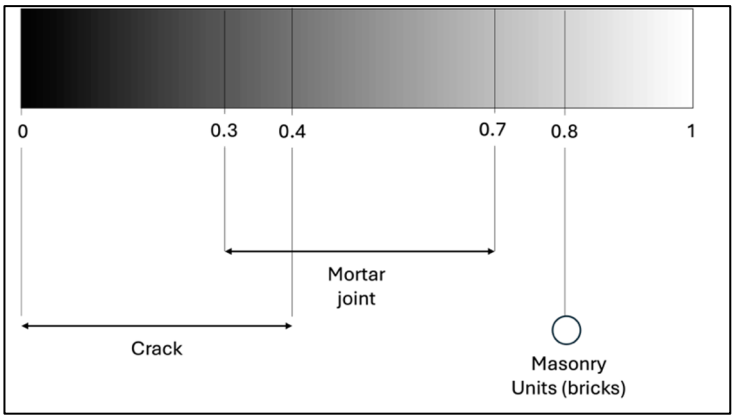

Fig. 2. Grayscale bar for colour selection. The range shown is from 0 to 1, where 0 is black and 1 is white.

An algorithm was developed to vary each generation variable 10 times within its range, and to generate 100000 different images to estimate the behaviour of the AI model for crack identification and understand the accuracy of the process. The methodology is summarised in
Fig. **3**, below.

The data flow represented shows the logic of the procedure used for the statistical analysis: the combination of variables is first done by defining the variables and their ranges, detailed in Table 2. Then the iteration with a nested for loop combines all the variables that change in their range, creating a wide imagery with all possible conditions to assess the model recognition capability even in the least likely scenarios. For each iteration, the variables of the generated synthetic image of masonry and crack are different (see the

Fig. **3** for reference). The ground truth image, consisting of the image of the crack alone on a white background is also generated, and used for later comparison. The generated images are processed by the AI model obtained from previous training and are used to create the segmented image output from the input crack image data. The segmented image is necessary for the subsequent evaluation of crack width and length.

The segmented image obtained after the inference with the model is the mask of the predicted crack image, which will be compared with the previously generated ground truth image to compute the IoU score between them. The IoU score equation is the same as the one used for the AI models test, Section **Erro! Fonte de referência não encontrada.**.

The closer the reference image is to the predicted image, the higher the IoU score, in this case the model performs as expected. Conversely, if the predicted image deviates greatly from the reference image, then the IoU score will be low and the model, with that parameter configuration, will have difficulty detecting the crack defect.

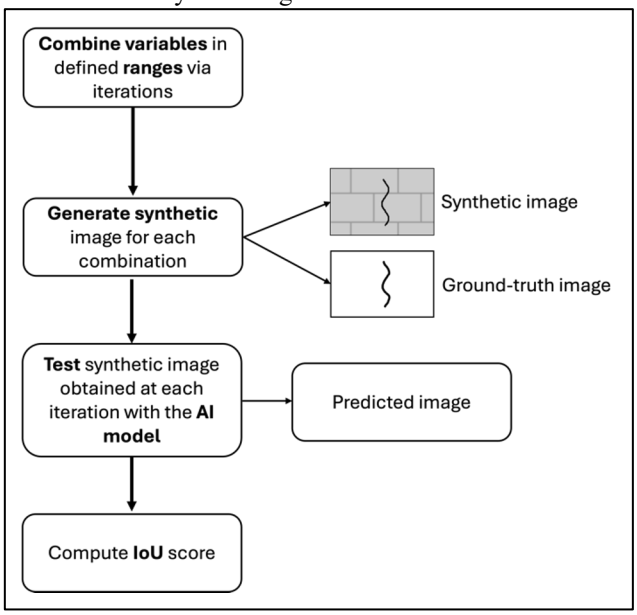

Fig. 3. Logic flow of data for evaluation of AI model via statistical analysis.

2.3 Measurement algorithm

The measurement algorithm for assessing the width and length of the crack utilizes the predicted mask obtained by the AI model. The model's accuracy must be sufficient to properly recognize the crack to achieve a good result.

The method starts by extracting contours from the image of the predicted crack. If more than one is detected, it filters them to extract only the larger ones, eliminating those smaller than 30% of the largest, based on the perimeter. This threshold has been experimentally established to avoid considering small areas erroneously detected as crack by the model. The remained contours are analysed separately to determine the feature measurements.

The image is divided into 200x200 pixel patches for further analysis, and finally, they will be merged for the visualization. For each patch, the central line of the crack is identified by fitting a polynomial curve (of 11th degree) through the contour points**Fig. 4**.

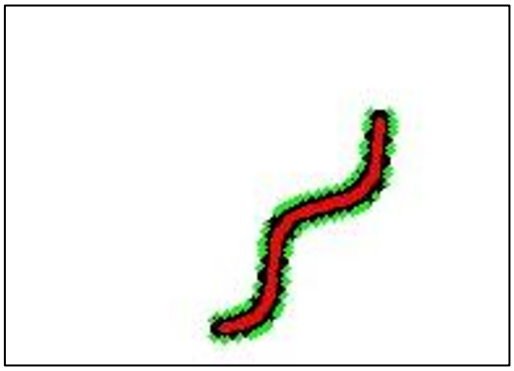

Fig. 4: Detected contours (green) and fitted central line (red).

A perpendicular line is constructed for each point along the central curve, extending to intersect both edges of the contours, Fig. 5.

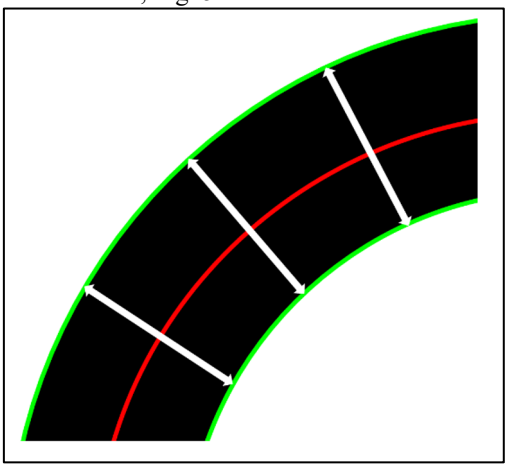

Fig. 5: Detected contours (green), fitted central line (red), and measurement line (white) of a part of synthetic crack.

The intersections delineate the width segment at each point along its length. The length of the width segment is calculated, providing a localised measure of the crack width. By averaging these widths over the entire length of the crack, an overall average width is obtained. The length of the crack is quantified by measuring the length of the central curve. By considering the extent of the crack along the curvilinear coordinate, a more complete representation of the actual size of the crack is obtained.

3 Results

3.1 Evaluation metrics for Synthetic Cracks Identification

From the statistical analysis 100000 IoU score values were obtained and evaluated. Examples are presented below to illustrate some of the best and worst combinations, along with the corresponding metrics.

The first two rows in Table 3 present the combinations from which very good metric were obtained, indicating perfect crack recognition, and the values of the variables used for generating the image. In fact, there is a high contrast between the colour of the crack and that

of the masonry joint, even though the thickness of the two entities is quite similar. The following two lines still represent good metrics, but the predicted segmented image loses a few pixels, due to the crack thickness being very small (1 pixel), as reported in the variable values. The next four rows of the table represent intermediate metrics, where the crack was confused with one of the masonry wall joint lines, along with the corresponding variable values used. Although the thickness of the cracks and the masonry joints are quite different in size, the colours of the two entities are not very contrasting, which ends up confusing the defect recognition pattern. The more similar the colours of the two entities are, the worse the result will be. Finally, the last rows of the table represent the lowest metrics, indicating the worst crack recognitions, along with the respective values of the variables. The worst cases occur precisely when the colours of the two entities coincide, causing significant confusion in recognizing the pixels that belong to the defect, as can be seen from the segmented image above. The legend below explains the abbreviations of the variables used in the analysis:

- Crack Thickness = CT,
- Joint Thickness = JT,
- Crack Colour = CC,
- Joint Colour = JC,
- Crack Rotation Angle = CRA.

Table 3. Correlation between output images and IOU score.

IoU Score	**Original Image**	**Predicted Segmented Image**	**Ground Truth**
99 %	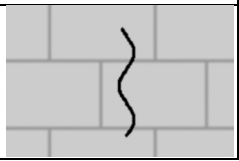	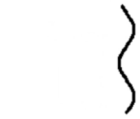	
CT = 2, JT = 3, CC = 0.08, JC = 0.6, CRA = 90			
93 %			
CT = 1, JT = 7, CC = 0.2, JC = 0.7, CRA = 70			
65 %	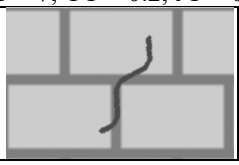	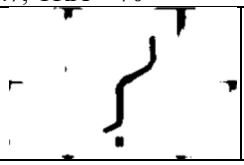	
CT = 4, JT = 10, CC = 0.3, JC = 0.5, CRA = 60			
62 %	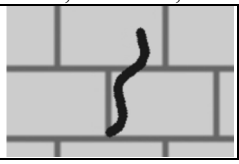	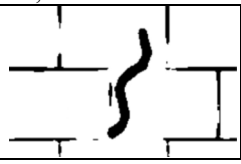	

CT = 8, JT = 6, CC = 0.1, JC = 0.4, CRA = 70			
25 %	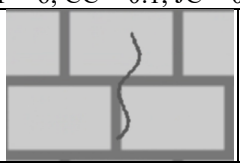	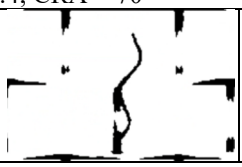	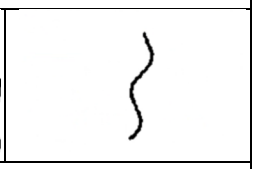
CT = 2, JT = 10, CC = 0.3, JC = 0.4, CRA = 80			
11 %		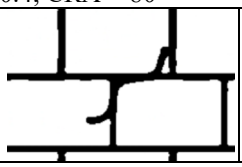	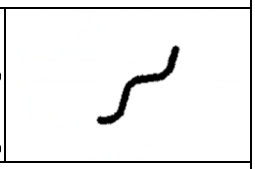
CT = 6, JT = 8, CC = 0.3, JC = 0.3, CRA = 40			

An analysis was then performed by setting the value of each variable within the previously defined range, one by one, while varying the others, and then averaging the IoU score. Ten IoU scores were calculated for each variable to individually assess its influence. Table 4 below, shows the average IoU (Av IoU) as a percentage by fixing the variable specified in the first column.

Table 4. Average IoU in percentage obtained fixing one variable at a time (first column on the left) and changing all the others. The rows alternate between the values of the variables in their respective ranges, and the calculated average IoU scores.

	Variables ranges – Average IoU scores									
CT [px]	1	2	3	4	5	6	7	8	9	10
Av IoU [%]	40.16	55.72	60.69	60.69	64.97	64.97	68.76	68.76	70.78	70.78
JT [px]	3	4	5	6	7	8	9	10	11	12
Av IoU [%]	79.27	73.69	63.76	61.68	60.00	57.83	56.88	58.07	58.40	56.69
CC [colour unit]	0	0.04	0.09	0.13	0.18	0.22	0.27	0.31	0.36	0.4
Av IoU [%]	71.65	70.5	68.73	66.84	64.79	62.43	60.11	57.48	54.05	49.7
JC [colour unit]	0.3	0.34	0.39	0.43	0.48	0.52	0.57	0.61	0.65	0.7
Av IoU [%]	23.36	24.98	29.44	42.12	59.51	74.08	88.63	93.7	94.92	95.54
CRA [deg]	0	10	20	30	40	50	60	70	80	90
Av IoU [%]	62.45	61.71	59.94	60.29	59.59	61.16	62.8	65.06	66.66	66.61

To better explain the approach used to represent Table 4, the first two rows are described in detailed in the following lines. In the first row, the value of crack thickness (CT) is given from 1 to 10. For CT = 1 all other previously defined parameters (JT, CC, JC, CRA) are

varied in their ranges, and the IoU score is calculated for each value. These values are then averaged to obtain an estimate of the metric as these parameters change while keeping a certain value of crack thickness fixed. The average IoU value obtained is 40%, which means that for a very small crack thickness, while varying all other values, the model does not recognize the defect optimally. Consequently, by setting CT = 2 and varying all parameters, the average IoU score is 55%, an increase from CT = 1. The average IoU score tends to increase as CT increases, reaching the maximum value of 70% for CT = 9 or at 10.

Applying the same logic used for the initial case under investigation, when considering the joint thickness (JT) within its range and varying all other parameters, the calculated average IoU score decreases as JT increases. By fixing the colour of the crack (CC) within its range and changing all other variables, the metrics worsen as the value of the colour in the respective range, increases, i.e., when it progresses from black to grey. Conversely, if the colour of the masonry joint is fixed each time and all other variables are changed, the metrics improve as the colour value increases within the previously defined range, i.e. from black to grey. In both latter cases described, this justifies how increasing the contrast between the two entities (crack and masonry joint) helps the model better recognize the defect. Finally, by fixing the rotation angles each time within the previously defined range, while all other parameters change, the metrics remain almost constant. In the Table 4, it is evident how the JC (joint colour) strongly affect the model's success in identification. In fact, when JC = 0.3, which is very close to black, there is low contrast with the CC values (crack colour), and the model becomes confused in the defect recognition, resulting in an average IoU score of 23.36 %. In contrast, when the contrast between CC and JC is high, the metrics become optimal, and the possibility of recognition can be as high as 90 %. The physical source of uncertainty (crack and masonry joint thickness and orientation) has little influence on model recognition. Certainly, if JT (joint thickness) is smaller and CT (crack thickness) is larger (or vice versa), recognition is facilitated, but the average metric value still remains around 60%. CRA (crack rotation angle) is the parameter that affects the model's recognition the least, as it consistently yields metrics around 60%.

3.2 Identification and measurement of cracking on masonry façades

This section presents a demonstration of the crack identification methodology developed and applied to a real case. This methodology was implemented in software that acquires the image of the component of interest, performs an inference with the model obtained from previous training, and then quantifies the width and the length of the crack, if identified.

Three different examples of masonry cracks are shown in Fig. 6: on the left are three images taken from three different masonry façades (a, b, c), on the right are the respective segmented images (d, e, f). The three images have the same pixel size. The contours of the cracks in Fig. 6 are in green to highlight the defects. The segmented images allow the number of pixels to be quantified to assess the extent of the defects. It can be noted that some small groups of pixels in the segmented images were not taken into account in the crack evaluation, because they were too small compared to the main object detected, and therefore discarded by the measurement algorithm, as mentioned in Section 2.3.

The measurements of defect sizes are given in Table 5 below. The width of the defect is the average width over the entire length, and therefore it is to be expected that defect c) is on average the thickest.

Table 5. Defects assessment for real case image acquisition.

Images	Width [pixel]	Length [pixel]
a)	16.16	310.95
b)	6.81	506.78
c)	20.92	371.33

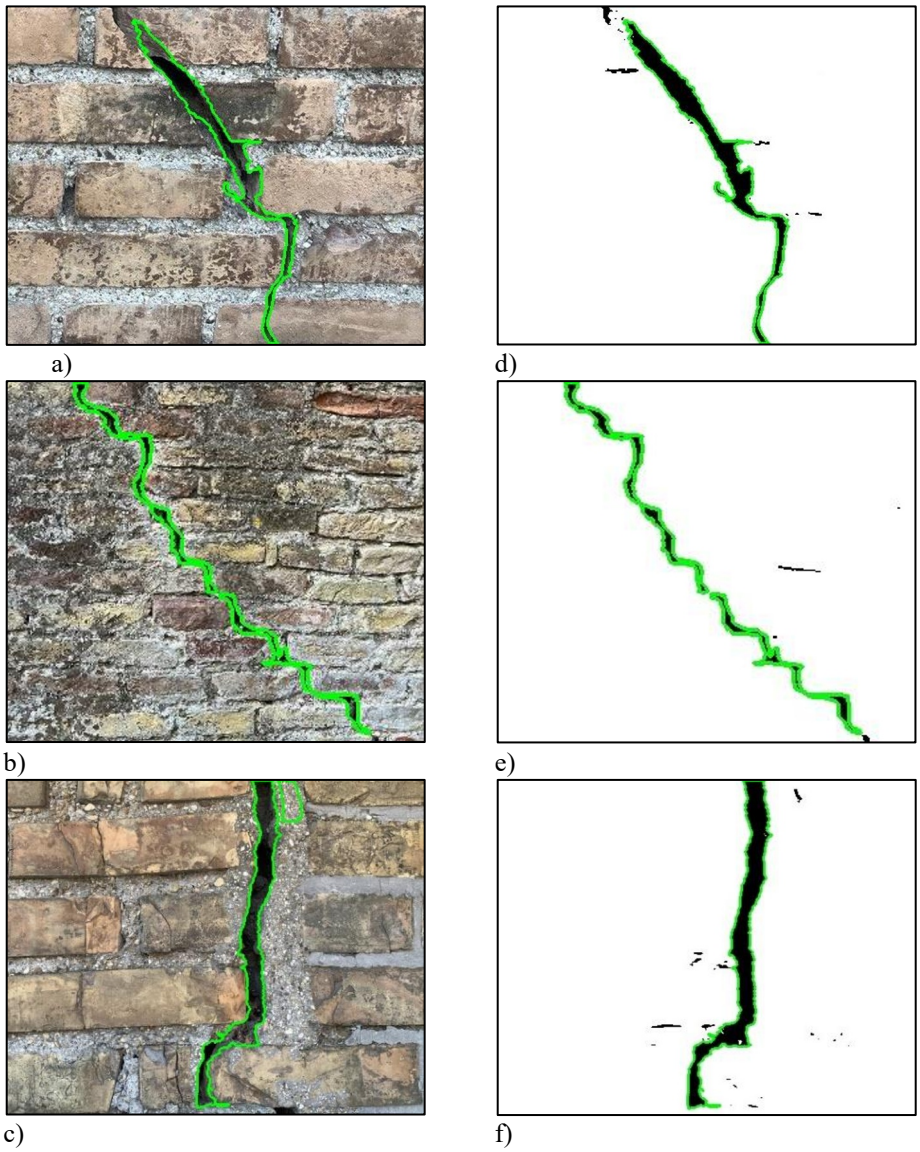

Fig. 6. Application of crack detection algorithm on masonry façades. a, b, c) Example of image acquired on a masonry surface. d, e , f) Image segmented from original image a, b, c) respectively.

4 Conclusions

The purpose of the study was to evaluate the metrological performances of an AI-based vision methodology developed for crack assessment on masonry façades and its sensitivity to physical source of uncertainty (crack and masonry joint thickness and orientation) and measurement source of uncertainty (image quality, and mainly contrast). To evaluate the influence of those sources, 100000 synthetic images have been generated to create a uniformly distributed database used as input to the AI-model to estimate its ability to successfully detect the defect. It has been found that the most influential source is the contrast between the crack and the mortar background and joint, represented by the crack and joint colour. Variation in joint colour was found to be the parameter that most affect the model's success in the crack identification, causing an uncertainty of 30%. Moreover, some parameters combination may cause confusion in the model due to the fact that the images used in the dataset are a mixture of images of cracks on masonry surfaces as well as on concrete surfaces whose textures differ from masonry elements. Despite this, when the contrast between the colours of the crack and the wall is high, one can distinguish the defect from the surface on which it arose. In contrast, when the contrast is low, it is very difficult for the model to identify the defect. To improve this aspect, one could expand the dataset by balancing it with more crack images on masonry and retrain the network to create a more consistent model. Although there are limitations of the model described above, the application of the software in real-world conditions is satisfactory; in fact, among the conditions considered in the evaluation of the model, unfavourable cases that are unlikely to be found in common constructions were considered to understand how the model reacts in these cases as well. This work, like many others from the literature that rely on the use of artificial intelligence models, may have limitations regarding the evaluation of the model's prediction, related to the type of image analyzed. The purpose of this work was to carry out a metrological analysis to understand which parameters most influence the defect recognition and the consequent measurement, in fact the recognition by the model plays a fundamental role for the efficient quantification of the defect by the algorithm. In this way, anyone who wants to use this type of approach is aware of its limitations.

Acknowledgements: The research presented in this paper has been funded by the European Union's Horizon 2020 research and innovation programme under grant agreement no. 958398, "BIM2TWIN: Optimal Construction Management & Production Control".

References

1. A. Hendry, B. Sinha and S. Davies, Design of masonry structures, E & FN Spon, 1997.
2. J. Ochsendorf, Collapse of Masonry Structures, University of Cambridge, 2002.
3. A. D'altri, V. Sarhosis, G. Milani, J. Rots, S. Cattari, S. Lagomarsino, E. Sacco, A. Tralli, G. Castellazzi and S. d. Miranda, "Modeling Strategies for the Computational Analysis of Unreinforced Masonry Structures: Review and Classification," Archives of Computational Methods in Engineering, 2020.
4. A. Soleymani, H. Jahangir and M. Nehdi, "Damage detection and monitoring in heritage masonry structures: Systematic review," Construction and Building Materials, 2023.
5. F. Pallares, M. Betti, G. Bartoli and L. Pallares, "Structural health monitoring (SHM) and Nondestructive testing (NDT) of slender masonry structures: A practical review," Construction and Building Materials, 2021.

6. Z. Orban, “UIC Project on assessment, inspection and maintenance of masonry arch railway bridges,” in 5th International Conference on Arch Bridges, 2007.
7. C. Gentile and A. Saisi, “ON-SITE INVESTIGATION AND DYNAMIC MONITORING FOR THE,” SAHC2014 – 9th International Conference on Structural Analysis of Historical Constructions F. Peña & M. Chávez (eds.), 2014.
8. A. Ellengberg, A. Kontsos, i. bartoli and A. Prandham, “Masonry Crack Detection Application of an Unmanned Aerial Vehicle,” COMPUTING IN CIVIL AND BUILDING ENGINEERING ©ASCE, 2014.
9. S. Hassani, U. Dackermann, M. Mousavi and J. Li, “A systematic review of data fusion techniques for optimized structural health monitoring,” Information Fusion, 2024.
10. E. Valero, A. Forster, F. Bosché, E. Hyslop, L. Wilson and A. Turmel, “Automated defect detection and classification in ashlar masonry walls using machine learning,” Automation in Construction, 2019.
11. Q. Qiu and D. Lau, “Real-time detection of cracks in tiled sidewalks using YOLO-based method applied to unmanned aerial vehicle (UAV) images,” Automation in Construction, 2023.
12. D. Dais, I. E. Bal, E. Smyrou and V. Sarhosis, “Automatic crack classification and segmentation on masonry surfaces using convolutional neural networks and transfer learning,” Automation in Construction, 2021.
13. M. Hallee, R. K. Napolitano, W. F. Reinhart and B. Glisic, “Crack Detection in Images of Masonry Using CNNs,” Sensors, 2021.
14. S. Katsigiannis, S. Seyedzadeh, A. Agapiou and N. Ramzan, “Deep learning for crack detection on masonry façades using limited data and transfer learning,” Journal of Building Engineering, 2023.
15. E. A. Shamsabadi, C. Xu and D. Dias-da-Costa, “Robust crack detection in masonry structures with Transformers,” Measurement, 2022.
16. L. M. Dang, H. Wang, Y. Li, L. Q. Nguyen, T. N. Nguyen, H. K. Song and H. Moon, “Deep learning-based masonry crack segmentation and real-life crack length measurement,” Construction and Building Materials, 2022.
17. X. Jin, M. Z. Haider, Y. Cui, J. G. Jang, Y. J. Kim, G. Fang and J. W. Hu, “Development of nanomodified self-healing mortar and a U-Net model based on semantic segmentation for crack detection and evaluation,” Construction and Building Materials, 2023.
18. N. Giulietti, P. Chiariotti and G. M. Revel, “Automated Measurement of Geometric Features in Curvilinear Structures Exploiting Steger’s Algorithm,” Sensors, 2023.
19. O. Ronneberger, P. Fischer and T. Brox, “U-Net: Convolutional Networks for Biomedical Image Segmentation,” in Lecture Notes in Computer Science, 2015.
20. S. Jadon, “A survey of loss functions for semantic,” 2020 IEEE Conference on Computational Intelligence in Bioinformatics and Computational Biology (CIBCB), 2020.
21. P. Yakubovskiy, Segmentation Models Documentation, Release 0.1.2, 2022.